

ShadowNet: A Secure and Efficient System for On-device Model Inference

Zhichuang Sun

Northeastern University

Ruimin Sun

Northeastern University

Changming Liu

Northeastern University

Amrita Roy Chowdhury

University of Wisconsin, Madison

Somesh Jha

University of Wisconsin, Madison

Long Lu

Ant Group and Northeastern University

Abstract

With the increased usage of AI accelerators on mobile and edge devices, on-device machine learning (ML) is gaining popularity. Consequently, thousands of proprietary ML models are being deployed on billions of untrusted devices. This raises serious security concerns about model privacy. However, protecting the model privacy without losing access to the AI accelerators is a challenging problem. In this paper, we present a novel on-device model inference system, ShadowNet. ShadowNet protects the model privacy with Trusted Execution Environment (TEE) while securely outsourcing the heavy linear layers of the model to the untrusted hardware accelerators. ShadowNet achieves this by transforming the weights of the linear layers before outsourcing them and restoring the results inside the TEE. The nonlinear layers are also kept secure inside the TEE. The transformation of the weights and the restoration of the results are designed in a way that can be implemented efficiently. We have built a ShadowNet prototype based on TensorFlow Lite and applied it on four popular CNNs, namely, MobileNets, ResNet-44, AlexNet and MiniVGG. Our evaluation shows that ShadowNet achieves strong security guarantees with reasonable performance, offering a practical solution for secure on-device model inference.

1 Introduction

On-device machine learning is gaining popularity as more and more AI accelerators are being used in mobile and embedded devices, such as NPU, GPU and Edge TPU [5]. Recent studies [43] have shown that thousands of mobile apps are using on-device machine learning (ML) for varied purposes, such as OCR, face recognition, liveness detection, ID card and bank card recognition, translation, and so on. The benefits of on-device machine learning are obvious. It avoids sending user’s private data to the cloud, saves the latency of back-and-forth communication and does not require a network connection. Many ML applications use on-device ML even for real-time tasks, such as rendering a live video stream, which is not possible with the traditional cloud-based ML on mobile devices.

However, with thousands of private models being deployed on billions of untrusted mobile devices, model theft is a real threat today. Attackers are not only technically capable of but also financially motivated to steal these models [43, 49]. Leakage of those proprietary models can cause severe financial loss to businesses – accurate models help companies maintain a competitive advantage and training the models requires a significant engineering effort (such as data collection, labeling and parameters tuning).

To make matters worse, existing proprietary models are found to be not well protected. As shown by Sun et al. in [43], 41% of the models are stored in plaintext and can be downloaded along with the application packages. Applications that protect the models (for example, by encrypting

the models) are still vulnerable to run-time attacks that can extract the decrypted models from the memory [43]. With 54% ML applications using GPUs for acceleration, it is even more complex to protect model privacy without losing access to the GPU accelerations.

Prior work on secure model inference can be classified into two types: trusted execution environment (TEE) based approaches and cryptography based approaches. Both of these techniques face unique challenges for on-device model inference. First, the TEE on mobile devices is designed for small critical tasks, such as key management, while model inference is a resource demanding task. Hence, supporting model inference on the limited resources (such as secure memory) of a TEE is challenging. Moreover, simply moving the model inference task inside the TEE would significantly increase the TCB size of the TEE. An additional problem is the loss of access to hardware accelerators. For cryptography based approaches, prior work uses either homomorphic encryption (HE) or multi-party computation (MPC) [10, 22, 30, 39]. However, HE based techniques are orders of magnitude slower than the state-of-the-art (non secure) model inference. MPC based approaches involve multiple participants requiring network connectivity which is not suitable for real-time tasks or off-line usage.

Table 1: Comparison of ShadowNet with Related Work

Works	Model Privacy	Mobile TEE	Performance	GPU Access
Slalom [45]			✓	✓
TensorScone [33]	✓		✓	
Graviton [48]	✓		✓	✓
CryptoNets [22]	✓			✓
TF Encrypted [10]	✓		✓	✓
OMG [17]	✓	✓	✓	
ShadowNet (Ours)	✓	✓	✓	✓

To this end, we design a novel secure model inference system, ShadowNet. The key idea of ShadowNet is based on the observation that the linear layers of CNNs usually take up 90% of the computational resources of the whole network [45]. ShadowNet offers a novel scheme that allows the heavy linear layers of the model to be securely outsourced to the untrusted world (including GPU) for acceleration without leaking the model weights. ShadowNet achieves it by transforming the weights of the linear layers before outsourcing them to the untrusted world, and restoring the results inside the TEE. The nonlinear layers are also kept secure inside the TEE.

We have built a prototype of ShadowNet based on TensorFlow Lite [9] and OP-TEE OS [35] and applied it on four popular CNNs, namely, MobileNets [26], ResNet-44 [25], AlexNet [32], and MiniVGG [42]. Our evaluation shows that the ShadowNet has performance that is comparable with the original models – it increases the model inference time by 61% for AlexNet (137ms) to 221% for ResNet-44 (51ms). The extra latency introduced by ShadowNet ranges from 48ms to 284ms for the above models which is still tolerable for the users. Table 1 compares ShadowNet with related prior work (see Section 8 for more details). Compared to the cryptography-based approaches [22] that are usually orders of magnitude slower, ShadowNet provides a practical solution for securing the on-device model inference. For instance, for a single image classification, CryptoNets takes around 570 seconds on PC while ShadowNet takes only a few hundreds of milliseconds on a smartphone. In summary, this paper makes the following contributions:

- We design a novel on-device model inference system, ShadowNet, which can protect the model privacy with a TEE while leveraging the untrusted hardware accelerators.
- We build an end-to-end ShadowNet prototype based on TensorFlow Lite with optimizations to support model inference inside a TEE with a small TCB.
- We present a formal security analysis of ShadowNet.

- Our evaluation on four popular CNNs, namely, MobileNets, ResNet-44, MiniVGG and AlexNet, demonstrates ShadowNet’s feasibility for real-world usage.

2 Background

In this section, we present the relevant background.

2.1 Convolutional Neural Network

Convolutional Neural Network (CNN) is a class of deep neural networks that is commonly used for analyzing visual images. A CNN consists of an input and an output layer, with a sequence of linear and nonlinear layers stacked in between. The linear layers include convolutional layers and fully connected layers. Some CNNs, such as ResNet and InceptionNet, introduce shortcut connections between convolutional layers, which create branches and merges in the network structure. Additionally, MobileNets introduces two new type of linear layers: pointwise convolution and depthwise convolution. The nonlinear layers include activation and pooling layers.

ShadowNet is based on the observation that most of the computation and the model weights are from the linear layers. ShadowNet applies linear transformation on the weights of the linear layers to obfuscate them. Consequently, the heavy linear layers can be outsourced to the untrusted hardware accelerators without leaking the original weights. The nonlinear layers remain unchanged and are computed inside the TEE.

2.2 Trusted Execution Environment

A trusted execution environment (TEE) is a secure area of the main processor. It guarantees the confidentiality and integrity of the code and data loaded inside [15].

Arm TrustZone [3] is a popular TEE implementation for mobile devices. It is a hardware feature available on both Cortex-A processors [13] (for mobile and high-end IoT devices) and Cortex-M processors [14] (for low-cost embedded systems). TrustZone renders a “Secure World”, an isolated environment with tagged caches, banked registers, and private memory for securely executing a stack of trusted software that includes a tiny OS and trusted applications (TA). In parallel runs the “Normal World” which contains the regular/untrusted software stack. Code in the Normal World, referred to as the client applications (CA), can invoke the TAs in the Secure World. A typical use of TrustZone involves a CA requesting a sensitive service from a TA, such as signing or encrypting a piece of data. Arm TrustZone has been widely used for security critical services, such as key management and Digital Rights Management(DRM) on smartphones.

OP-TEE (Open Portable Trusted Execution Environment) [35] is an open-source trusted OS running inside Arm TrustZone. It supports a wide variety of mobile devices ranging from Arm Juno Board, Raspberry Pi 3 to a series of Hikey boards. It is also integrated with AOSP to run alongside Android OS. OP-TEE OS usually reserves a small part of DRAM (for example, 32MB) as secure memory to minimize the performance impact on the Normal World applications.

We choose Hikey960 [1] as our development board which has Arm TrustZone support. It runs Android P as the Normal World OS and OP-TEE as the Secure World OS [8]. ShadowNet runs the transformed linear layers of the model in the Normal World and uses a CA to communicate with the TA in the Secure World, which runs the other layers of the model securely.

security critical services, such as managing encryption keys. The memory reserved for the TEE OS is limited. For example, only 14 MB is available for trusted applications of OP-TEE OS on Hikey960 Dev Board while the model size of AlexNet is 242 MB. Hence, it is not feasible to run the high resource-demanding model inference task inside the TEE. Second, current TEEs do not include the GPU/NPU in the secure domain. Hence, we would lose access to hardware acceleration. Third, the model inference framework would also significantly increase the TCB of TEE, risking the security of the whole system.

3.4 Our Solution: ShadowNet

Key Idea: ShadowNet is based on the observation that the linear layers of CNNs occupy the majority of the model parameters and model inference time. This is in line with previous research, such as Slalom [45]. For example, the linear layers of MobileNets occupy around 95% of the model parameters and 99% of the model inference time. The key idea of ShadowNet is to apply linear transformation on the weights of the linear layers and outsource them to the untrusted world. In this way, we can leverage the hardware accelerators without trusting them. ShadowNet then restores the results inside the TEE. The other nonlinear layers are also kept secure inside the TEE.

With this design, ShadowNet’s security is rooted in the TEE, meeting the first design goal. ShadowNet does not introduce any heavy cryptographic operations and our evaluation shows that ShadowNet has reasonable overhead – this meets our second design goal. Finally, ShadowNet is still able to use the hardware accelerators which meets the third design goal. Additionally, ShadowNet solves the technical challenges of mobile TEEs by maintaining low memory usage and a small TCB.

Example Application: We use a simple example to show how ShadowNet works on a typical CNN, as depicted in Figure 1. The example CNN is a stack of convolutional layers, and each convolutional layer (*conv*) is followed by a batch normalization (*bn*) layer and a ReLU6 (*relu6*) activation layer.

For each convolutional layer *conv*, the ShadowNet transformation works in four steps: (1) adds a mask layer to the input; (2) replaces the original *conv* layer with a transformed *conv*’ layer; (3) adds a *linear transformation* layer to restore the result of the *conv*’; (4) unmask the input. The combination of *conv*’+*linear transformation* is equivalent to *conv* in the original CNN. The combination of *mask*+*conv*’+*linear transformation*+*unmask* is also equivalent to *conv* in the original CNN. The batch normalization layer and ReLU6 layer remain unchanged.

The *mask* and *unmask* layers in step (1) and step (4), respectively, are introduced to prevent the adversary from observing the original input and output of the outsourced linear layers. We discuss how these layers are implemented in Section 4.2. Step (3) and step (4) show the high level ideas of how ShadowNet works on a convolutional layer. Note that the *conv*’ layer has 76 kernels instead of 64 kernels. This is due to the *obfuscation ratio*, a tunable parameter in ShadowNet. In Section 4.3, we will explain the rationale behind the choice of this number and how to generate the weights for *conv*’ layer and *linear transform* layer. We will also discuss how ShadowNet transforms the other type of linear layers, namely, pointwise convolutional, depthwise convolutional and dense/fully connected layers.

In summary, ShadowNet offers a novel model inference system that protects the model weights with a TEE while leveraging the untrusted hardware for acceleration. ShadowNet achieves its goal by transforming the heavy linear layers’ weights and masking their input before outsourcing them to the untrusted world and restoring the results inside the TEE. The nonlinear layers are also kept secure inside the TEE.

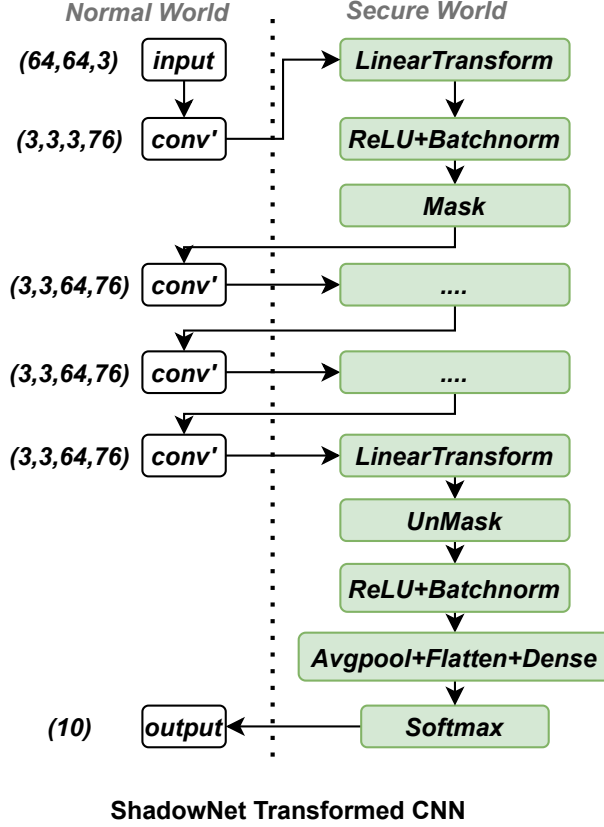


Figure 2: **An example of ShadowNet transformed CNN.**

This example has four convolution layers. The input and output shape as well as the weights shape of the convolutional layers are marked in the figure. Observe that for the first layer, *only the output* is masked. For the last layer, *only the input* is masked. This is because according to our threat model, the input to the first layer (model input) and the output of the last layer (model output) is already known to the adversary.

4 ShadowNet

In this section, we introduce ShadowNet. First, we explain how ShadowNet applies linear transformation on a broad class of linear layers, namely convolutional, pointwise convolutional, depthwise convolutional, and dense/fully connected layers. Next, we discuss the mask layer for input/output privacy. Finally, we describe an optimized implementation of the linear transformations for ShadowNet.

Notations: Here, we introduce the notations we use for the rest of the paper. X and Y denote the input and output of a convolutional layer. X' and Y' denote the transformed/masked input and output. $\hat{W} = [\hat{w}_1, \dots, \hat{w}_n]$ represents a transformed convolution filter corresponding to the original convolution filter $W = [w_1, \dots, w_n]$ where $\hat{w}_i(w_i)$ denotes a masked (original) convolution kernel. Additionally, all random values (used for masking and the transformations) in ShadowNet are drawn uniformly at random from an interval $[-t, t]$ for some $t^2 \in \mathbb{R}$. Also, for a positive integer $n \in \mathbb{Z}_{>0}$, $[n]$ denotes the set $\{1, 2, \dots, n\}$.

4.1 Transformation of Linear Layers

ShadowNet relies on linear transformation to obfuscate the weights of the linear layers.

² t is sufficiently large and kept secret.

Linear Transformation: Linear transformation is a function f defined on vector space V and T over the same field R , $f : V \rightarrow T$. In our scenario, R is the field of real number. For any two vectors $u, v \in V$ and any scalar $c \in \mathbb{R}$, the following two conditions are satisfied:

$$\begin{aligned} \text{additivity} : f(u + v) &= f(u) + f(v) \\ \text{homogeneity} : f(cu) &= cf(u) \end{aligned} \quad (1)$$

Convolutional Layer: The convolutional layer is the core building block of a CNN. The parameters of the convolutional layer consists of a set of learnable kernels. Each kernel is characterized by the width, height and depth of the receptive field. The depth must be equal to the number of channels (depth) of the input feature map. For the *conv* layer from our example CNN in Figure 1, the input shape is (224, 224, 3) where 3 is the depth. The convolutional layer of the example CNN has 64 kernels. The shape of the convolution kernel is (3, 3, 3), which corresponds to the receptive field's height, width and depth.

Formally, the convolution operation on a given image I with kernel w can be described as below, where h, b, d represents the height, width and depth of the kernel w , and (x, y) refer to the coordinates in the two-dimensional output feature map.

$$\text{Conv}(I, w)_{x,y} = \sum_{i=1}^h \sum_{j=1}^b \sum_{k=1}^d w_{i,j,k} I_{x+i-1, y+j-1, k} \quad (2)$$

Before transformation, the convolutional layer can be described as follows, where X and Y denote the input and output, respectively and $W = [w_1, \dots, w_n]^T$ is the convolution filter.

$$Y = \text{Conv}(X, W^T) \quad (3)$$

Let $F = [f_1, \dots, f_n]$ be a random filter such that each $f_i, i \in [n]$ has the same shape as w_i . Additionally, let $\lambda_i, i \in [n]$ be a random scalar. Conceptually, the linear transformation on the convolutional layer in ShadowNets works as follows.

$$\begin{aligned} \hat{W}^T &= W^T \cdot \Lambda + F \\ \Rightarrow [\hat{w}_1, \dots, \hat{w}_n] &= [w_1, \dots, w_n] \begin{bmatrix} \lambda_1 & & \\ & \ddots & \\ & & \lambda_n \end{bmatrix} + [f_1, \dots, f_n] \end{aligned} \quad (4)$$

Thus, each of the kernels are transformed as follows

$$\hat{w}_i = \lambda_i w_i + f_i \quad (5)$$

Hence, from the transformation Equation (4) and the properties of linear transformation Equation (1), we have:

$$\begin{aligned} \text{Conv}(X, \hat{W}^T) &= \text{Conv}(X, W^T \cdot \Lambda + F) \\ &= \text{Conv}(X, W^T) \cdot \Lambda + \text{Conv}(X, F) \end{aligned} \quad (6)$$

So we can compute $\text{Conv}(X, \hat{W}^T)$ on the untrusted GPU and restore the output Y with the following formula inside the TEE:

$$Y = (\text{Conv}(X, \hat{W}^T) - \text{Conv}(X, F)) \cdot \Lambda^{-1} \quad (7)$$

Note that the computation of $\text{Conv}(X, F)$ is done in the Normal World. We discuss how we implement the above transformation in an optimized manner in ShadowNet in Section 4.3.

Pointwise Convolutional Layer: The pointwise convolutional layer is a type of convolution whose kernel height and width are both 1. The scheme for the standard convolutional layer can be directly applied to the pointwise convolutional layer.

Depthwise Convolutional Layer: Depthwise convolution is a type of convolution where we apply a single convolutional kernel for each input channel. The number of input channels and the number of kernels are the same. For a given image I and kernel w , the depthwise convolution $DWConv$ on input channel c can be described as follows where h and b represent the height and width of the kernel w , respectively, and (x, y) refer to the coordinates in the two-dimensional output feature map. Note that the kernel w is a two-dimensional matrix.

$$DWConv(I^{(c)}, w)_{x,y} = \sum_{i=1}^h \sum_{j=1}^b w_{i,j} I_{x+i-1, y+j-1}^{(c)} \quad (8)$$

The original depthwise convolutional layer is described as follows, where x_i represents i -th channel of input X .

$$\begin{aligned} Y &= DWConv(X, W) \\ &= [DWConv(x_1, w_1), \dots, DWConv(x_n, w_n)] \end{aligned} \quad (9)$$

For depthwise convolutional layers, ShadowNet applies linear transformations on both the input and the kernels. Specifically, we (1) shuffle the sequence of input/kernel channels and (2) obfuscate each input/kernel channel with a random scalar as detailed below.

Assume the input has n channels, so the depthwise convolutional layer has n kernels, one per channel. Let w_i represent the i -th kernel of the convolution filter W , where $W = [w_1, w_2, \dots, w_n]^T$. Let $(\lambda_1, \dots, \lambda_n)$ be a set of random scalars and $\pi \in S_n$ (S_n is the group of permutations on $[1, \dots, n]$) be a random permutation. Additionally, let P_π be a $n \times n$ permutation matrix corresponding to π ($P_\pi(i, j) = 1$ if $\pi(i) = j$, and 0 otherwise). We scale and shuffle the sequence of the kernels in W with Λ as follows:

$$\Lambda = \begin{bmatrix} \lambda_1 & & \\ & \ddots & \\ & & \lambda_n \end{bmatrix} P_\pi \quad (10)$$

We apply the same permutation to shuffle the input channels. The input transformation matrix A is defined as follows:

$$A = \begin{bmatrix} \frac{1}{\lambda_1} & & \\ & \ddots & \\ & & \frac{1}{\lambda_n} \end{bmatrix} P_\pi \quad (11)$$

Thus, for identity matrix I , we have:

$$A \cdot \Lambda^T = I \quad (12)$$

The transformation on the input X and weights W are described as follows, where $\hat{W} = [\hat{w}_1, \dots, \hat{w}_n]^T$ is the transformed weights:

$$\begin{aligned} \hat{W}^T &= W^T \cdot \Lambda \\ X' &= X \cdot A \end{aligned} \quad (13)$$

Let $Y' = \text{DWConv}(X', \hat{W}^T)$. It is easy to see that:

$$Y' = [\text{DWConv}(x_1, w_1), \dots, \text{DWConv}(x_n, w_n)] P_\pi \quad (14)$$

Let P_π^{-1} be the inverse of P_π . We can restore the correct result with the following equation:

$$Y = Y' \cdot P_\pi^{-1} \quad (15)$$

Note that both the transformation of the input and the restoration of the result are performed inside the TEE while the depthwise convolution on the transformed filter can be outsourced to the untrusted GPU.

Dense/Fully Connected Layer: The dense or fully connected layer is a common layer used in neural networks as well as CNNs. The dense layer connects every input node to every output node. It can be implemented as a pointwise convolutional layer. For example, a dense layer connect n input to m output can be viewed as a pointwise convolutional layer that has m kernels of size $(1, 1, n)$. We can apply the same linear transformation which we described for the standard convolutional layer.

4.2 Layer Input/Output Privacy

We introduce the mask/unmask layer to protect the input X and output Y of the convolutional layers.

Mask Layer: The mask layer adds a random mask to the input of a convolutional layer, which is outsourced to the Normal World. Note that, in a typical CNN, the output of a convolutional layer output will be the input for the next layer. In an off-line phase, ShadowNet generates random masks M of the same shape as X inside the TEE. The masked input X' is defined as follows:

$$X' = X + M \quad (16)$$

X' is outsourced to the Normal World for the convolutional layer with filter W . Note that a fresh mask is used for every convolutional layer and for every round of model inference.

Unmask Layer: After obtaining the masked output Y' from the Normal World, the TEE restores the original value as follows:

$$Y = Y' - \text{Conv}(M, W) \quad (17)$$

where TEE pre-computes and stores the value of $\text{Conv}(M, W)$ in an off-line phase. This masking step is in line with that of Slalom [45].

Recall from our threat model (Section 3.2) that the adversary already knows $Y = \mathcal{M}(X)$ where \mathcal{M} is the CNN model. Hence, the input to the first layer (model input) and the output of the last layer (model output) is *not* masked. This is depicted in Figure 2.

4.3 Optimized Implementation

In this section, we describe how ShadowNet implements the linear transformation for the convolutional layers.

Recall from our discussion in Section 4.1 that F acts as a mask that protects the weights of the kernels. However, the TEE needs access to $\text{Conv}(X, F)$ for restoring Y (Equation (7)) – the extra computation for $\text{Conv}(X, F)$ is a performance overhead. This introduces a performance/security trade-off which is tackled in ShadowNet as follows:

- First, we select $r \in \mathbb{R}, r > 1$. We refer to r as the *obfuscation ratio* and it is a parameter for tuning the performance/security trade-off. We elaborate on this later in this section.

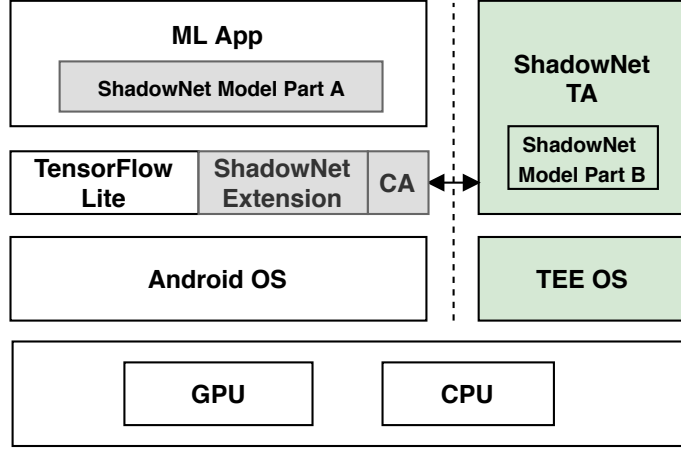


Figure 3: **The system architecture of Shadownet on mobile platforms.** Color grey shows the part modified by ShadowNet in the Normal World. Color green shows the part in the Secure World. The ShadowNet model part A and B refer to linear and nonlinear part respectively.

- Select at random $F = [f_1, \dots, f_{m-n}]$ where $m = \lceil r \cdot n \rceil$. Each f_i has the same shape as that of the kernels of W .
- Select a set of n random scalars $(\lambda_1, \dots, \lambda_n)$.
- Compute

$$W' = [\lambda_1 w_1 + f'_1, \dots, \lambda_n w_n + f'_n, f_1, \dots, f_{m-n}]^T \quad (18)$$

where f'_i 's are randomly chosen from F . Repetitive choice is allowed here as $m - n$ might be smaller than n .

- Stores an index matrix C where $C[i] = j$ iff $f'_i = f_j$.
- Finally, shuffle W' with a random permutation matrix P_π for $\pi \in S_m$.

$$\hat{W}^T = W'^T P_\pi \quad (19)$$

All of the above steps can be pre-computed securely in an off-line phase. With this transformation, we can easily recover the convolution results with the inverse of the permutation matrix P_π , the index matrix C and the random scalars $(\lambda_1, \dots, \lambda_n)$. Conceptually, the recovery process can be implemented as a pointwise convolution with n filters of shape $(1, 1, m)$.

Intuitively, the permutation π prevents the adversary from distinguishing between the kernels in \hat{W} that correspond to F and the ones that correspond to (transformed) W . Clearly, higher the values of r , better is the security and higher is the computational overhead. The formal security and performance analysis, as a function of r , is presented in Sections 6.4 and 6.3, respectively. Note that ShadowNet applies the aforementioned transformation to every convolutional layer of the CNN.

5 Implementation

5.1 Overview of the ShadowNet prototype

We have implemented the ShadowNet prototype as an end-to-end on-device model inference system, as shown in Figure 3. It contains the ML mobile application, the TensorFlow Lite runtime library with extensions for ShadowNet, the ShadowNet client application (CA) and the ShadowNet trusted

application (TA). The ShadowNet models are split into Part A and Part B, denoting the Normal World and the Secure World, respectively.

During a model inference task, TensorFlow Lite handles the linear layers in the Normal World. For the nonlinear layers, the ShadowNet CA sends commands to the TA, which handles them inside the Secure World and passes the results back.

5.2 Model Conversion

Model conversion takes two steps. First, we replace all the linear layers with their corresponding ShadowNet transformed layers. All the other layers are kept unchanged. Second, we split the transformed model into Part A and Part B. An illustrative example is presented in Figure 4.

In the first step, we introduce four new layers: LinearTransform, ShuffleChannel, PushMask, PopMask. LinearTransform applies linear transformation on the input. ShuffleChannel shuffles the sequence of the channels and also scales each channel in the input. PushMask (PopMask) adds (removes) the mask from its input.

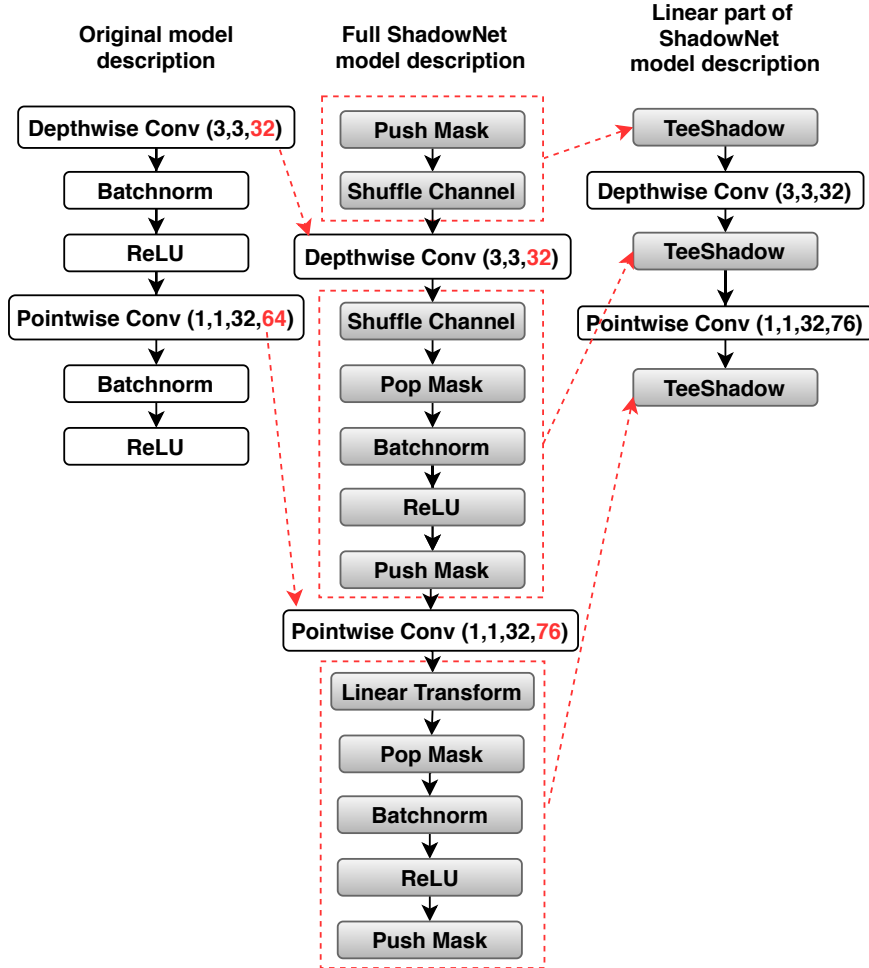


Figure 4: **An example of ShadowNet model conversion ($r = 1.2$).** In the first step, the linear layers are transformed. The pointwise convolutional layer’s weight shape changes from (1, 1, 32, 64) to (1, 1, 32, 76), where $76 = 64 \times 1.2$. In the second step, the linear layers remain unchanged and the nonlinear layers are replaced with a placeholder TeeShadow.

There are four types of linear layers in CNNs: convolutional, pointwise convolutional, depth-wise convolutional and fully connected/dense. Among them, pointwise convolutional and fully

connected/dense can be treated as standard convolution during the conversion phase (as explained in Section 4.1). The rules for the first step of the model conversion are:

- Every convolutional layer (including pointwise convolutional and fully connected/dense layers) is replaced with four layers: PushMask layer, transformed convolutional layer, LinearTransform layer and PopMask layer.
- Every depthwise convolutional layer is replaced with five layers: PushMask layer, ShuffleChannel layer, transformed depthwise convolutional layer, ShuffleChannel layer and PopMask layer.
- The nonlinear layers remain unchanged.

In the second step, we introduce the TeeShadow layer between the linear layers which serves as a placeholder for all the interposed nonlinear layers. During a model inference task, the TeeShadow layer simply switches to the Secure World to handle the nonlinear layers and returns back to the Normal World. Note that we treat all the newly added ShadowNet layers (LinearTransform, ShuffleChannel, PushMask and PopMask) as nonlinear layers and put them in the Secure World.

For CNNs with shortcuts, such as ResNet [25], the TeeShadow layer needs to merge inputs from different branches. We present an illustration in Appendix B to show how we handle shortcuts in ShadowNet.

Hence, the overall rule is simple: the linear layers remain unchanged; the nonlinear layers are replaced with a TeeShadow layer, as shown in Figure 4. Model Part A contains weights for the transformed linear layers which is stored in the Normal World. Model Part B contains weights for all the others layers that reside in the Secure World.

5.3 Adding ShadowNet Support in TensorFlow Lite

ShadowNet introduces four *operations* that are not supported in the TensorFlow Lite framework, namely, **LinearTransform**, **ShuffleChannel**, **AddMask** and **TeeShadow**. Both PushMask and PopMask layers are implemented via AddMask. To add support for ShadowNet, we extend TensorFlow Lite as follows:

- Add ShadowNet related operations as CustomOps for TensorFlow.
- Add Keras **Layer** support for the above operations to provide Keras API.
- Add TensorFlow Lite implementation of the CustomOps to support model inference on mobile devices.

The extension is based on TensorFlow 2.2 which was the most recent version at the time of our implementation. To support CustomOp for TensorFlow, we added 563 LOC in Python, 924 LOC in C++; to support TensorFlow Lite, we added 774 LOC in C++.

5.4 ShadowNet CA and TA

The ShadowNet CA and TA work as follows. During the initialization phase, the ShadowNet CA starts a secure session with the TA and loads the ShadowNet Model Part B into the TA. Before each round of model inference, the ShadowNet CA loads pre-computed weights for mask layers into the TA. During a model inference task, the ShadowNet CA passes the parameters from the TeeShadow operation to the TA and fetches results from it. ShadowNet TA performs the model inference task for the nonlinear layers shadowed by the TeeShadow operation as shown in Figure 4.

There are several challenges in implementing the ShadowNet TA. We share two of them here: TA’s memory management and performance optimization.

Optimizing TA’s Memory Management: The TEE OS has a limited memory reserved for the TA. Without careful memory management, the TA would exhaust the memory and crash. We tackle this challenge as follows. First, we use static memory allocation in the TA to avoid fragmentation. Specifically, for a given model, the memory needed for each layer is predictable and can be allocated statically. Dynamically allocating memory with *malloc* will cause fragmentation of the TA memory. Second, we do not allocate buffer for each layer’s output. Instead, we allocate two big buffers and rotate them to save memory.

Optimizing TA’s Performance: Implementing the TA in OP-TEE has many restrictions. For example, OP-TEE only supports C; we lose access to popular compute libraries, such as Eigen [7] and Arm Compute Lib [2] in C++. Additionally, OP-TEE lacks a math library. Hence, we had to find efficient implementation of mathematical functions, such as *sqrt*, *exp*, or *tanh*, for the activation layers.

Table 2: Optimizations of the TA (with MobileNets model)

Optimizations	Exec. Time (ms)
Baseline (Static mem. alloc)	1500
(1) Neon sqrt	300
(2) Cache friendly	245
(3) Optimize loop sequence	205
(4) Preload weights	100
(5) Neon for Batchnorm, AddMask	90
(6) Neon for ReLU6	81

Note: The optimizations are applied in a sequence. For example, the 81 ms is the execution time inside the TA (excluding mask weights reloading time) when optimizations (1) to (6) are all applied.

Initially, we ported the nonlinear layers from the Darknet [38], a deep learning framework for desktop written in C. However, the resulting TA was very slow on our Arm64 Dev Board. Hence, we propose the following optimizations to bring the performance at par with that of TensorFlow Lite.

- Using Arm Neon to optimize the *sqrt* implementation in the Batchnorm layer.
- Swapping the inner and outer loops to support cache-friendly data access.
- Moving repetitive computation out of the loops and pre-computing it.
- Pre-loading all weights to avoid repetitive loading.
- Using Neon multiply+add instructions to optimize the Batchnorm and AddMask layers.
- Using Neon minimum/maximum instructions to optimize the activation layers, such as the ReLU6 layer.

Table 2 shows the execution times for our proposed optimization for the MobileNets TA. An illustration of the *sqrt* optimization is presented in Appendix A

We also changed the size of the TEE OS reserved secure memory from 16MB to 64MB to accommodate a larger Part B. Additionally, we changed the reserved shared memory size from 2MB to 8MB, which is the region for the CA and TA to exchange parameters. These changes only require a few lines of configurational code in the TEE OS and Arm Trusted Firmware. No change is required in the Normal World OS, such as Android/Linux. In total, we added 480 LOC in C for the CA and 2100 LOC in C for the TA.

ShadowNet Accuracy Evaluation on MobileNets and ResNet-44

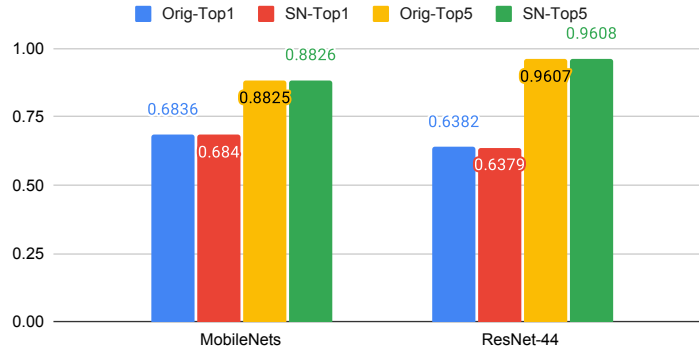


Figure 5: **Prediction accuracy evaluation of ShadowNet.** Orig-Top1 refers to the original model’s top-1 accuracy, SN-Top1(5) refers to the ShadowNet transformed model’s top-1(5) accuracy.

6 Evaluation

We evaluate ShadowNet on four popular machine learning models: MobileNets, ResNet-44, AlexNet, and MiniVGG. We perform the evaluation on the Hikey960 board equipped with the Kirin 960 SoC which features 4 Cortex A73 + 4 Cortex A53 Big.Little CPU architecture, ARM Mali G71 MP8, and 3GB LPDDR4 SDRAM. We run Android P in the Normal World and OP-TEE OS 3.9.0 in the Secure World.

Our evaluation focuses on four questions:

- Correctness: Does ShadowNet produce the same result as the original model?
- Efficiency: What is the overhead introduced by ShadowNet?
- Obfuscation Ratio: What is the impact of the obfuscation ratio on the correctness and performance of ShadowNet?
- Security: What is the formal security guarantee of ShadowNet?

6.1 Correctness

We evaluate the correctness of ShadowNet transformation along two metrics: prediction accuracy and consistency. Prediction accuracy checks whether ShadowNet has the same accuracy as that of the original model. Consistency checks whether ShadowNet is consistent with the original model on the same input. Figure 5 shows our evaluation results on two popular models: MobileNets and ResNet-44. MobileNets is evaluated on the ImageNet-2012 dataset [40] with 50K images. ResNet-44 is evaluated on the CIFAR-10 dataset [31] with 10K images. We observe that ShadowNet has negligible impact on the model prediction accuracy. For consistency, ShadowNet’s Top1 prediction is 99.02% consistent with the original model for MobileNets and 99.56% for ResNet-44. Hence, ShadowNet is consistent with the original model.

6.2 Efficiency

We evaluate the efficiency of ShadowNet on MobileNets, ResNet-44, AlexNet, and MiniVGG. We use the model inference time as our metric which measures the time span between feeding an image and getting the classification result.

Experimental Highlights: Our evaluation shows that:

ShadowNet Performance Evaluation on Different Models(ms)

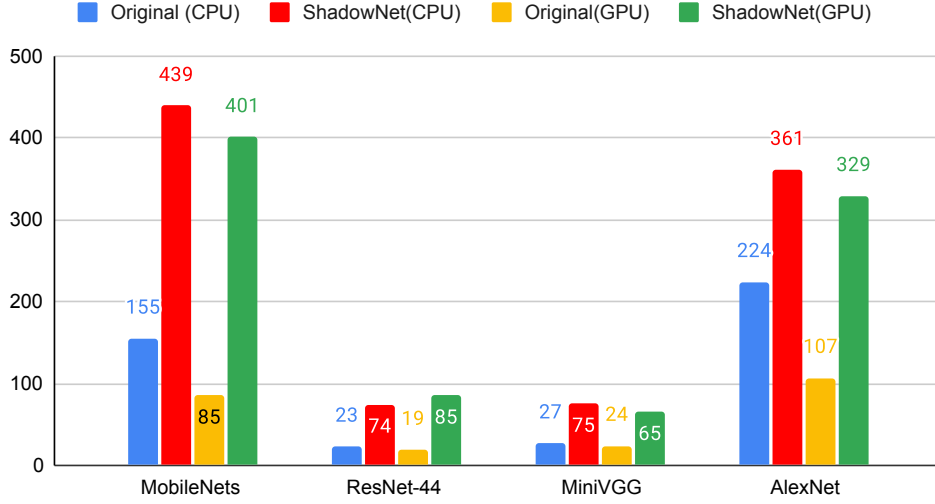


Figure 6: **ShadowNet performance evaluation.** We evaluate ShadowNet on four representative CNN models: MobileNets, ResNet-44, MiniVGG and AlexNet. For each model, we measure the model inference time for one image on four different settings: original model on CPU, ShadowNet model on CPU, original model on GPU and ShadowNet model on GPU. We report the mean of 100 trials.

- ShadowNet results in a reasonable overhead, increasing the model inference time from 61% to 221% (or 48ms to 281ms).
- GPU acceleration can reduce the model inference time in three of the models by 10ms to 38ms (or 9% to 13%). However, the GPU’s benefit is not as significant as it is for the original models. This can be improved by optimizing the CPU/GPU communications in ShadowNet.

Methodology: We use the TF Lite Android image classifier Demo application [11] developed by Google to evaluate the end-to-end model inference time. We evaluate ShadowNet under different settings: (1) the original model on CPU; (2) the ShadowNet transformed model on CPU; (3) the original model on GPU; (4) the ShadowNet transformed model on GPU. The obfuscation ratio is set at 1.2. We discuss the impact of obfuscation ratio in Section 6.3. Figure 6 shows the model inference time under the above settings.

ShadowNet Performance on CPU: Compared with the original model in CPU mode, ShadowNet incurs an overhead of 284ms (183%), 51ms (221%), 48ms (178%) and 137ms (61%) for MobileNets, ResNet-44, MiniVGG and AlexNet, respectively. The overhead is reasonable as ShadowNet needs to refresh the masks for each round of model inference. Table 3 shows the model weights size before and after ShadowNet transformation. For example, for MobileNets model, the weights of the mask layers has a size of 37MB which takes around 200ms to update them. The Normal World and Secure World (TEE) switches can also cause extra overhead. The size of the weights of the mask layers of ResNet-44 is 3.3MB and it takes around 18ms to update them. AlexNet has the biggest model size, 242MB, but the size of the weights for its mask layers is less than 5MB. As a result, its performance is less affected by ShadowNet (61%). ShadowNet increases the model inference time by 221% for ResNet-44 which requires significantly more world switches (44 in total).

As for the application user, although the additional 48ms to 284ms increases the latency, the impact on user experience is reasonable, especially for small models. We test this by running Demo to detect objects in real-time. For example, Demo processes six images per second with the

Table 3: ShadowNet model size change.

Model Size(MB)		MobileNets	ResNet-44	MiniVGG	AlexNet
Original Model	<i>Conv</i>	17	2.43	20	242
	<i>Other</i>	0.175	0.029	0	0.015
ShadowNet Model	<i>Conv</i>	20	2.92	24	291
	<i>Other</i>	37	3.3	2	5

Model weights are divided into two parts: *Conv* layers’ weights (standard convolutional, pointwise convolutional, depthwise convolutional and dense layers) and *Other* layers’ weights (AddMask, LinearTransform, ShuffleChannel, Batchnorm). Among the *Other* layers, the weights of the AddMask layer occupy the maximum space for ShadowNet models.

original MobileNets model and 2.5 images per second with ShadowNet. For small models, such as MiniVGG, the extra 48ms latency is almost imperceptible to users.

Performance Impact from GPU: Running on GPU reduces model inference time by 38ms (9%), 10ms (13%) and 32ms (9%) for MobileNets, MiniVgg and AlexNet, respectively. The time increases by 9ms (12%) for ResNet-44. Overall, we see some benefit of GPU acceleration for ShadowNet but it is not as significant as it is for the original models. This is due to the following reasons. First, ShadowNet requires splitting the model inference between the CPU (TEE mode) and the GPU. The interleaving between the CPU and the GPU causes extra overhead for repeated setting up of GPU jobs. This switching overhead, in fact, nullifies the performance gain from the GPU for ResNet-44. Second, the GPU speedup ($\sim 2X$) on our evaluation board is significantly less than the GPU speedup in the cloud. Mobile GPU acceleration for on-device ML is still a developing research area [6]. Thus, GPU’s impact on ShadowNet can be improved via optimized GPU/CPU switching and/or more powerful hardware AI accelerators.

6.3 Obfuscation Ratio

In this section, we evaluate how the model accuracy, model size and model inference time vary with increasing r . The result is shown in Figure 7 for MobileNets. We observe that both *top1* and *top5* accuracy remain almost unchanged as r is varied from 1.0 to 2.0. This shows that ShadowNet’s accuracy does not depend on the obfuscation ratio. Another observation is that the model size increases linearly with r and so does the model inference time. This is intuitive because both the weight size and the amount of computation for the convolutional layers grow linearly with r .

6.4 Security Analysis

In this section, we present the formal security analysis of ShadowNet.

Let us consider a CNN with k standard convolution layers where W_i denotes the convolution filter for the i -th layer. Additionally, X_i (Y_i) denote the input (output) for the i -th layer. For a transformed filter \hat{W} , let $\mathcal{F}(\hat{W})$ represent the set of filters that could have been transformed to \hat{W} , i.e., the set of possible pre-images for \hat{W} . We call this the *feasible set* for \hat{W} . The exact construction of $\mathcal{F}(\hat{W})$ is detailed in Appendix D. The view of the adversary is equivalent to that of the Normal World and is illustrated in Figure 8.

²We are ignoring the batch normalization and ReLU layers for simplicity and a worst case analysis for security. In practice, the adversary can only observe $\hat{X}_i = G(Y_{i-1}) + M_i$ where $G(\cdot)$ represents the non-linear layers. This adds additional complications for the adversary. For instance, negative values cannot be reversed for ReLU activation layers.

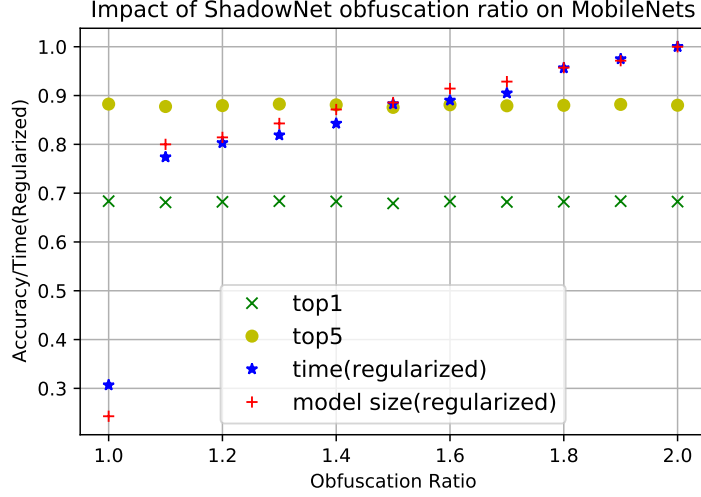


Figure 7: **Analysis of performance with varying obfuscation ratio.** We measure the change in model accuracy (top1 and top5), model size (regularized) and model inference time (regularized) with the obfuscation ratio, r , (ranging from 1 to 2) for MobileNets. Here, $r = 1$ refers to the original model and is treated as the baseline.

Theorem 1. For a CNN with k convolutional layers and a given view of the normal world³ $View_{Normal} = (X_1, Y_k, \hat{W}_1, \dots, \hat{W}_k, X'_2, \dots, X'_k)$, we have:

$$\forall i \in [k], \forall (W', W'') \in \mathcal{F}(\hat{W}_i) \times \mathcal{F}(\hat{W}_i) \quad (20)$$

$$\Pr[W_i = W' | View_{Normal}] = \Pr[W_i = W'' | View_{Normal}] \quad (21)$$

Proof Sketch. Every input/output pair for the intermediate layers $i \in [2, k-1]$ is masked and hence, cannot be used to reconstruct the convolution filters. For the first (last) layer, the output (input) is masked which also prevents any reconstruction of the true weights for W_1 (W_k). The rest of the proof follows trivially from the construction of the feasible sets $\mathcal{F}(W_i)$. The full proof is presented in Appendix D. \square

The above theorem states that, on observing a transformed filter \hat{W}_i , corresponding to any convolutional layer i , an adversary cannot distinguish between two filters that belong to its *feasible set*. Thus, the feasible sets act as cloaking regions for the original weights. Intuitively, larger the value of the obfuscation ratio r , greater is the size of the feasible set and consequently, better is the security. Concretely, $\mathcal{F}(\hat{W}_a) \supset \mathcal{F}(\hat{W}_b)$ where $m_a = |\hat{W}_a| > |\hat{W}_b| = m_b$ (equivalently, $r_a > r_b$).

Based on Theorem 1, we present the following conjecture:

Conjecture 1. Let q be the number of queries required for a model stealing attack with access to just the querying API, i.e., $Y = \mathcal{M}(X)$ ⁴ and some information about the model architecture (such as, number and type of convolutional layers). Let q' be the number of queries required for an attack on ShadowNet. We conjecture that q' is of the order of $O(q)$.

³For simplicity and ease of exposition, we assume that the TEE is perfectly secure, i.e., it acts as a trusted third party, and that it has access to a true random number generator. In practice, we would have to use a pseudorandom number generator (PRNG) with some security parameter κ . We can account for this by assuming a computationally bounded adversary and considering an additional $\text{negl}(\kappa)$ term in the Equation (21) where $\text{negl}(\cdot)$ is a negligible function.

⁴This corresponds to access to (X_1, Y_k) from Figure 8.

Attacker's view of ShadowNet model inference	
Input: x	
View:	$Conv'_i, 1 \leq i \leq L$ $I_{i-1} - u_{i-1} + m_{i-1}$ $I_0 = x, m_0 = \text{input_mask},$ $u_0 = 0, u_1 = \text{input_unmask},$ $y = F(x), \text{output of the model}.$
Goal of Attacker:	Find weights of $Conv_i, 1 \leq i \leq L.$

Figure 8: **Formalization of the attacker's goal** $y = F(x)$ refers to the CNN with L convolutional layers. Given input x , the model's output is y . I_{i-1} refers to the input from previous layer $i - 1$, m_{i-1} and u_{i-1} refers to the mask/unmask at layer $i - 1$. For each $Conv'_i$ layer, the attacker can observe the masked input $I_{i-1} - u_{i-1} + m_{i-1}$, and the weights of $Conv'_i$. Attacker's goal is to find the original weights of $Conv_i$.

We conjecture that with ShadowNet, an adversary cannot do anything significantly better than a standard black-box⁵ model stealing attack [28, 37, 46]. Our reasoning is based on the fact the feasible sets for the transformed weights are sufficiently large – this provides sufficient cloaking region for the original weights. In other words, an adversary cannot learn anything useful about the original weights by observing the ShadowNet transformed weights. We provide an illustration and empirical evidence in support of our conjecture as follows.

Illustration: In order to study the advantage an adversary might have in ShadowNet, over a black-box model stealing attack, we assume that the adversary reuses the transformed weights to build an equivalent CNN.

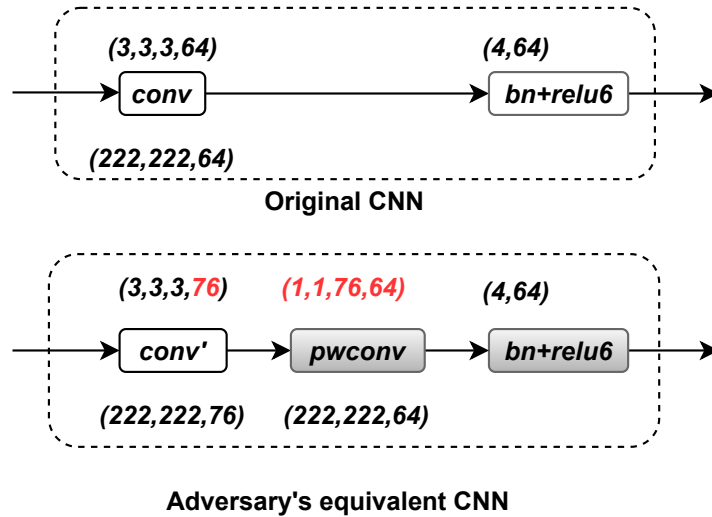


Figure 9: **The equivalent CNN architecture needed to be trained by an adversary.** The red color marks the weights shape of the layers with unknown parameters that the adversary has to train. The weights shape is marked on top of the box and the output shape is marked under the box.

⁵with some extra information about the architecture as stated in Conjecture 1

Consider the example CNN from Figure 1 – the minimum equivalent CNN that reuses the transformed weights is shown in Figure 9. As mentioned before in Section 4.3, the linear transformation layer is essentially a pointwise convolutional layer and we use *pwconv* to represent it inside the TEE. Note that the mask/unmask layers are not needed to construct the equivalent CNN.

We use the number of learnable parameters to assess the difficulty of training a CNN. In our example, the block in the original CNN has $3 \times 3 \times 3 \times 64 + 4 \times 64 = 1,984$ parameters while the block in the adversary’s equivalent CNN has $76 \times 64 + 4 \times 64 = 5,120$ parameters to be trained. Here, 4×64 learnable parameters are due to the batch normalization (*bn*) layer. There are 76 kernels in the *conv*’ layer and this number can be configured via the obfuscation ratio, which is set to $r = 1.2$ in our example ($76 = 64 \times 1.2$). In fact, even for $r = 1$, the minimum allowed value, the adversary’s CNN has more learnable parameters ($64 \times 64 + 4 \times 64 = 4,480$). Hence, we conjecture that the adversary gains no advantage by training an equivalent CNN with the transformed weights from ShadowNet.

Empirical Analysis: We empirically evaluate our conjecture on an example CNN with four convolutional layers as shown in Figure 2. The adversary’s equivalent CNN is presented in Appendix C. First, we copy the ShadowNet transformed weights for *conv*’ layers to the adversary’s equivalent CNN. Next, we mark the adversary’s *conv*’ layers as non-trainable and only train the other layers. Figure 10 shows the learning curves for varying training epochs. We observe that the adversary’s model has significantly lower accuracy than the victim’s model after the same number of training epochs. In fact, the adversary’s model performs worse than the random baseline where the weights of the non-trainable convolutional layer are randomly initialized. This shows that the ShadowNet transformed weights contain no useful information about the original weights and the adversary gains no advantage by reusing the transformed weights. Additionally, it slowed down the training for the adversary as more parameters need to be trained.

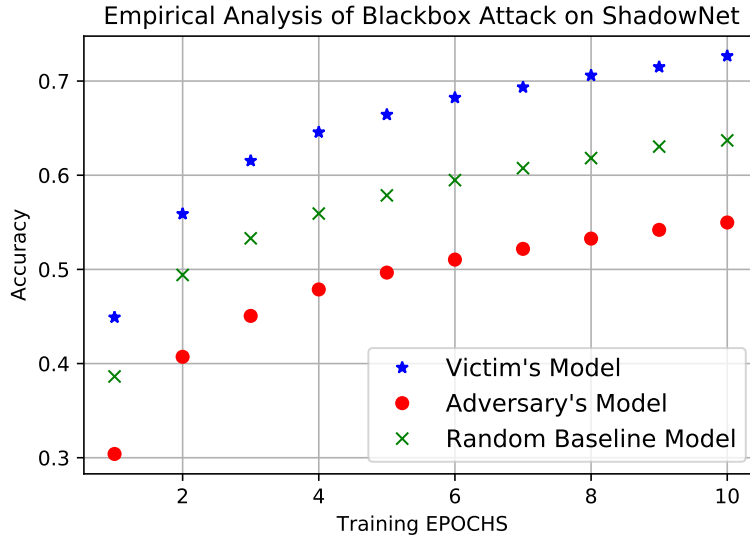


Figure 10: **Empirical analysis of training the equivalent CNN by Adversary.** The *Adversary* copies the transformed weights from the *Victim*’s model and treats the hidden layers as black-box. We compare the training curve of both the *Victim*’s model and the *Adversary*’s model and evaluate whether the *Adversary* can gain any advantage by reusing the *Victim*’s transformed weights (from ShadowNet). The *Random Baseline* model shares the same structure as that of the *Adversary*’s model except that the weights of its non-trainable convolutional layers are randomly initialized. The experiments are performed on the CIFAR-10 dataset using SGD optimization with a learning rate of 0.01.

7 Discussion

Support for CNNs and RNNs: We have applied our ShadowNet prototype on MobileNets, ResNet-44, AlexNet and MiniVGG, covering a broad range of CNN architectures. For example, MobileNets contains depthwise convolutional and pointwise convolutional layers. ResNet-44 contains shortcuts between different convolutional layers. Following the same transformation rules, ShadowNet can be applied on InceptionNet, DenseNet and so on.

ShadowNet can also be used on RNNs, such as LSTMs. For LSTMs, we can apply linear transformation for the fully connected layers while keeping the pointwise operations and activation layers inside the TEE. This is because ShadowNet only supports linear layers with fixed weights. If the weights are changing dynamically, then the transformation can not be performed off-line. Hence, we need to move the pointwise operations on cell states to the TEE as it changes over time.

Support for Cloud Platform: ShadowNet can be applied for secure model inferencing in the cloud as well. For this, the ShadowNet CA/TA needs to be changed to support cloud TEE, such as SGX. Compared to other designs that perform model inferencing inside SGX [12, 33] ShadowNet would be more efficient in using the SGX memory and would benefit from the co-located GPUs for acceleration.

Layerwise ShadowNet: ShadowNet transformations can be applied on each convolutional layer independently. Hence, an alternative strategy for implementation is to selectively apply ShadowNet on a few layers that are considered to be the most sensitive. We call this scheme Layerwise ShadowNet. Clearly, Layerwise ShadowNet would result in better performance.

The rationale behind Layerwise ShadowNet is backed up by research on transferable learning [50] which shows that the bottom layers of the CNN models contain features that are more specific to the training dataset. Hence, these features are more sensitive than the generalized features in the top layers. Thus, Layerwise ShadowNet offers a trade-off for balancing security and performance.

Quantized Models: Quantization is a popular trend on mobile devices [27]. Our current implementation for ShadowNet does not support quantized models. Quantized models usually use 8-bit integer for weight parameters. The computation on the ShadowNet transformed weights overflows easily which might affect the correctness of the transformed model when quantized. We leave the extension of ShadowNet to support quantized models as a future work.

8 Related Work

Existing research on secure ML covers both end devices and cloud-based solutions. Offline Model Guard (OMG) [17] provides a secure model inference framework for mobile devices based on SANCTUARY [18], a user space enclave based on Arm TrustZone. OMG allows the model inference framework to run fully inside the SANCTUARY enclave to protect the model privacy. MLCapsule [24] also deploys the model on the client side to protect the user input from being sent to the untrusted cloud. Additionally, it runs the model inference inside SGX to prevent the model from being leaked to the client. DarknetTZ [36] is a secure machine learning framework built on top of Arm TrustZone. It allows a few selected layers to run inside the TEE to protect part of the model. OMG, MLCapsule and DarknetTZ do not support secure GPU acceleration and have a large TCB size. ShadowNet has a comparatively smaller TCB size and allows secure outsourcing of the linear layers to the GPU. Graviton [48] proposes TEE extension for GPU hardware, thus allowing GPU tasks, such as ML, to run securely on the GPU. It requires hardware changes on the GPU. Secloak [34] partitions the GPU into Secure World with Arm TrustZone to run GPU tasks securely at a high performance penalty. ShadowNet does not change the GPU hardware or partition the GPU into the Secure World.

Research on secure ML in the cloud is an active area. TensorSCONE [33] proposes a secure ML framework that runs on the untrusted cloud. TensorSCONE integrates TensorFlow with the secure Linux container technology, SCONE [16], guarded by SGX. TF Trusted [12] leverages custom operations to send gRPC messages into the Intel SGX device via Google Asylo [4] where the model is then run by Tensorflow Lite. Running model inference inside TEE faces performance challenges due to limited memory and lack of GPU acceleration. These works require more resource from the TEE than ShadowNet and do not support GPU acceleration.

Slalom [45] outsources the linear layers to the GPU for acceleration with masked inputs while keeping the other layers inside SGX. Slalom protects the user input privacy but not the model weights⁶ w.r.t. the untrusted server while ShadowNet protects the model weights. YerbaBuena [23] partitions the model into frontnets (such as the first layer) and backnets, and executes the frontnets inside SGX. This protects the user input from being leaked to the untrusted cloud. SecureNets [20] transforms both the input and the linear layer’s weights into matrices and applies matrix transformations [41] before sending them to the untrusted cloud for acceleration. It is unclear whether SecureNets supports depthwise convolution and convolution with stride. ShadowNet does not require transforming input and weights into matrices and is compatible with existing linear operations.

There are also secure ML systems using cryptographic primitives. CryptoNets [22] applies HE on neural networks and runs model inference on the encrypted data to protect user input privacy. Jiang et. al [29] presents a solution for encrypting a matrix using HE to protect both the user data and the model. TF Encrypted [10] enables training and prediction over encrypted data via MPC and HE. SafetyNets [21] designs an interactive protocol that allows clients to verify the correctness of a class of DNNs running on the untrusted cloud. ShadowNet’s performance is orders of magnitude better than such cryptographic approaches. For instance, for a single image classification, CryptoNets takes ~ 570 seconds on PC while ShadowNet takes less than a second on a smartphone.

To ensure the integrity of model weights, Uchida et. al [47] and Zhang et. al [51] embed watermarks into deep neural model parameters while training the models. DeepAttest [19] encodes fingerprint in DNN weights to prevent weight modification. These works do not prevent weight leakage.

9 Conclusion

In this paper, we have proposed ShadowNet, a secure on-device model inference system that protects the model privacy with a TEE while leveraging the untrusted hardware for acceleration. The key idea of ShadowNet is to apply linear transformation on the weights of the linear layers and outsource them to the untrusted world. In this way, ShadowNet leverages the hardware accelerators without trusting them and restores the results inside the TEE. We have implemented an end-to-end prototype of ShadowNet on TensorFlow Lite and OP-TEE with optimizations to support secure model inference with a small TCB. Our evaluation on four popular CNNs, namely, MobileNets, ResNet-44, MiniVGG and AlexNet demonstrates ShadowNet’s practical feasibility on real-world datasets.

⁶Slalom outlines a conceptual way for protecting the model privacy from clients – however, no concrete implementation and performance analysis is provided.

References

- [1] HiKey 960 . <https://www.96boards.org/product/hikey960/>.
- [2] Arm Compute Library. <https://www.arm.com/why-arm/technologies/compute-library>.
- [3] Arm TrustZone. <https://developer.arm.com/ip-products/security-ip/trustzone>.
- [4] Asylo, An open and flexible framework for enclave applications. <https://asylo.dev/>.
- [5] Coral: An ecosystem for local AI. <https://coral.ai/about-coral/>.
- [6] Coral: An ecosystem for local AI. <https://blog.tensorflow.org/2019/01/tensorflow-lite-now-faster-with-mobile.html>.
- [7] Eigen. http://eigen.tuxfamily.org/index.php?title=Main_Page.
- [8] OP-TEE AOSP support. <https://optee.readthedocs.io/en/latest/building/aosp/aosp.html>.
- [9] Tensorflow lite. <https://www.tensorflow.org/lite>.
- [10] TF Encrypted. <https://github.com/tf-encrypted/tf-encrypted>.
- [11] TF Lite Android Image Classifier App Example. <https://github.com/tensorflow/tensorflow/tree/r2.2/tensorflow/lite/java/demo>.
- [12] TF Trusted. <https://github.com/dropoutlabs/tf-trusted>.
- [13] TrustZone for Cortex-A. <https://www.arm.com/why-arm/technologies/trustzone-for-cortex-a>.
- [14] TrustZone for Cortex-M. <https://www.arm.com/why-arm/technologies/trustzone-for-cortex-m>.
- [15] Wiki: Trusted Execution Environment. https://en.wikipedia.org/wiki/Trusted_execution_environment.
- [16] Sergei Arnautov, Bohdan Trach, Franz Gregor, Thomas Knauth, Andre Martin, Christian Priebe, Joshua Lind, Divya Muthukumaran, Dan O’keeffe, Mark L Stillwell, et al. {SCONE}: Secure linux containers with intel {SGX}. In *12th {USENIX} Symposium on Operating Systems Design and Implementation ({OSDI} 16)*, pages 689–703, 2016.
- [17] Sebastian P Bayerl, Tommaso Frassetto, Patrick Jauernig, Korbinian Riedhammer, Ahmad-Reza Sadeghi, Thomas Schneider, Emmanuel Stapf, and Christian Weinert. Offline model guard: Secure and private ml on mobile devices. *DATE 2020*, 2020.
- [18] Ferdinand Brasser, David Gens, Patrick Jauernig, Ahmad-Reza Sadeghi, and Emmanuel Stapf. Sanctuary: Arming trustzone with user-space enclaves. In *NDSS*, 2019.
- [19] Huili Chen, Cheng Fu, Bitu Darvish Rouhani, Jishen Zhao, and Farinaz Koushanfar. Deepattest: an end-to-end attestation framework for deep neural networks. In *Proceedings of the 46th International Symposium on Computer Architecture*, pages 487–498, 2019.

- [20] Xuhui Chen, Jinlong Ji, Lixing Yu, Changqing Luo, and Pan Li. Securenets: Secure inference of deep neural networks on an untrusted cloud. In *Asian Conference on Machine Learning*, pages 646–661, 2018.
- [21] Zahra Ghodsi, Tianyu Gu, and Siddharth Garg. Safetynets: Verifiable execution of deep neural networks on an untrusted cloud. In *Advances in Neural Information Processing Systems*, pages 4672–4681, 2017.
- [22] Ran Gilad-Bachrach, Nathan Dowlin, Kim Laine, Kristin Lauter, Michael Naehrig, and John Wernsing. Cryptonets: Applying neural networks to encrypted data with high throughput and accuracy. In *International Conference on Machine Learning*, pages 201–210, 2016.
- [23] Zhongshu Gu, Heqing Huang, Jialong Zhang, Dong Su, Ankita Lamba, Dimitrios Pendarakis, and Ian Molloy. Yerbabuena: Securing deep learning inference data via enclave-based ternary model partitioning. *arXiv preprint arXiv:1807.00969*, 2018.
- [24] Lucjan Hanzlik, Yang Zhang, Kathrin Grosse, Ahmed Salem, Max Augustin, Michael Backes, and Mario Fritz. Mlcapsule: Guarded offline deployment of machine learning as a service. *arXiv preprint arXiv:1808.00590*, 2018.
- [25] Kaiming He, Xiangyu Zhang, Shaoqing Ren, and Jian Sun. Deep residual learning for image recognition. In *Proceedings of the IEEE conference on computer vision and pattern recognition*, pages 770–778, 2016.
- [26] Andrew G Howard, Menglong Zhu, Bo Chen, Dmitry Kalenichenko, Weijun Wang, Tobias Weyand, Marco Andreetto, and Hartwig Adam. Mobilenets: Efficient convolutional neural networks for mobile vision applications. *arXiv preprint arXiv:1704.04861*, 2017.
- [27] Benoit Jacob, Skirmantas Kligys, Bo Chen, Menglong Zhu, Matthew Tang, Andrew Howard, Hartwig Adam, and Dmitry Kalenichenko. Quantization and training of neural networks for efficient integer-arithmetic-only inference. In *Proceedings of the IEEE Conference on Computer Vision and Pattern Recognition*, pages 2704–2713, 2018.
- [28] Matthew Jagielski, Nicholas Carlini, David Berthelot, Alex Kurakin, and Nicolas Papernot. High-fidelity extraction of neural network models. *arXiv preprint arXiv:1909.01838*, 2019.
- [29] Xiaoqian Jiang, Miran Kim, Kristin Lauter, and Yongsoo Song. Secure outsourced matrix computation and application to neural networks. In *Proceedings of the 2018 ACM SIGSAC Conference on Computer and Communications Security*, pages 1209–1222, 2018.
- [30] Chiraag Juvekar, Vinod Vaikuntanathan, and Anantha Chandrakasan. {GAZELLE}: A low latency framework for secure neural network inference. In *27th {USENIX} Security Symposium ({USENIX} Security 18)*, pages 1651–1669, 2018.
- [31] Alex Krizhevsky, Vinod Nair, and Geoffrey Hinton. Cifar-10 (canadian institute for advanced research).
- [32] Alex Krizhevsky, Ilya Sutskever, and Geoffrey E Hinton. Imagenet classification with deep convolutional neural networks. *Advances in neural information processing systems*, 25:1097–1105, 2012.
- [33] Roland Kunkel, Do Le Quoc, Franz Gregor, Sergei Arnautov, Pramod Bhatotia, and Christof Fetzer. Tensorscone: A secure tensorflow framework using intel sgx. *arXiv preprint arXiv:1902.04413*, 2019.

- [34] Matthew Lentz, Rijurekha Sen, Peter Druschel, and Bobby Bhattacharjee. Secloak: Arm trustzone-based mobile peripheral control. In *Proceedings of the 16th Annual International Conference on Mobile Systems, Applications, and Services*, pages 1–13, 2018.
- [35] Linaro. Open Portable Trusted Execution Environment. <https://www.op-tee.org/>.
- [36] Fan Mo, Ali Shahin Shamsabadi, Kleomenis Katevas, Soteris Demetriou, Ilias Leontiadis, Andrea Cavallaro, and Hamed Haddadi. Darknetz: Towards model privacy at the edge using trusted execution environments. In *ACM MobiSys 2020*.
- [37] Nicolas Papernot, Patrick McDaniel, Ian Goodfellow, Somesh Jha, Z Berkay Celik, and Ananthram Swami. Practical black-box attacks against machine learning. In *Proceedings of the 2017 ACM on Asia conference on computer and communications security*, pages 506–519, 2017.
- [38] Joseph Redmon. Darknet: Open source neural networks in c. <http://pjreddie.com/darknet/>, 2013–2016.
- [39] M Sadegh Riazi, Christian Weinert, Oleksandr Tkachenko, Ebrahim M Songhori, Thomas Schneider, and Farinaz Koushanfar. Chameleon: A hybrid secure computation framework for machine learning applications. In *Proceedings of the 2018 on Asia Conference on Computer and Communications Security*, pages 707–721, 2018.
- [40] Olga Russakovsky, Jia Deng, Hao Su, Jonathan Krause, Sanjeev Satheesh, Sean Ma, Zhiheng Huang, Andrej Karpathy, Aditya Khosla, Michael Bernstein, Alexander C. Berg, and Li Fei-Fei. ImageNet Large Scale Visual Recognition Challenge. *International Journal of Computer Vision (IJCV)*, 115(3):211–252, 2015.
- [41] Sergio Salinas, Changqing Luo, Weixian Liao, and Pan Li. Efficient secure outsourcing of large-scale quadratic programs. In *Proceedings of the 11th ACM on Asia Conference on Computer and Communications Security*, pages 281–292, 2016.
- [42] Karen Simonyan and Andrew Zisserman. Very deep convolutional networks for large-scale image recognition. *arXiv preprint arXiv:1409.1556*, 2014.
- [43] Zhichuang Sun, Ruimin Sun, and Long Lu. Mind your weight (s): A large-scale study on insufficient machine learning model protection in mobile apps. *arXiv preprint arXiv:2002.07687*, 2020.
- [44] Christian Szegedy, Wei Liu, Yangqing Jia, Pierre Sermanet, Scott Reed, Dragomir Anguelov, Dumitru Erhan, Vincent Vanhoucke, and Andrew Rabinovich. Going deeper with convolutions. In *Proceedings of the IEEE conference on computer vision and pattern recognition*, pages 1–9, 2015.
- [45] Florian Tramer and Dan Boneh. Slalom: Fast, verifiable and private execution of neural networks in trusted hardware. *arXiv preprint arXiv:1806.03287*, 2018.
- [46] Florian Tramèr, Fan Zhang, Ari Juels, Michael K Reiter, and Thomas Ristenpart. Stealing machine learning models via prediction apis. In *25th {USENIX} Security Symposium ({USENIX} Security 16)*, pages 601–618, 2016.
- [47] Yusuke Uchida, Yuki Nagai, Shigeyuki Sakazawa, and Shin’ichi Satoh. Embedding watermarks into deep neural networks. In *Proceedings of the 2017 ACM on International Conference on Multimedia Retrieval*, pages 269–277, 2017.

- [48] Stavros Volos, Kapil Vaswani, and Rodrigo Bruno. Graviton: Trusted execution environments on gpus. In *13th {USENIX} Symposium on Operating Systems Design and Implementation ({OSDI} 18)*, pages 681–696, 2018.
- [49] Mengwei Xu, Jiawei Liu, Yuanqiang Liu, Felix Xiaozhu Lin, Yunxin Liu, and Xuanzhe Liu. A first look at deep learning apps on smartphones. In *The World Wide Web Conference*, pages 2125–2136, 2019.
- [50] Jason Yosinski, Jeff Clune, Yoshua Bengio, and Hod Lipson. How transferable are features in deep neural networks? In *Advances in neural information processing systems*, pages 3320–3328, 2014.
- [51] Jialong Zhang, Zhongshu Gu, Jiyong Jang, Hui Wu, Marc Ph Stoecklin, Heqing Huang, and Ian Molloy. Protecting intellectual property of deep neural networks with watermarking. In *Proceedings of the 2018 on Asia Conference on Computer and Communications Security*, pages 159–172, 2018.

Appendix A Optimizing the sqrt function

Table 4: Performance of different *sqrt* implementation.

<i>Sqrt</i> Impl.	Time(ms)	S/H	Algorithm	CFLAG
GNU libc	3.53	S	IEEE754	Default
Newlib	13.78	S	IEEE754	-O2
Our TA	194.04	S	Newton	-Os
Arm VFP	10.86	H	unknown	Default
Arm Neon	6.62	H	Newton	Default

Note: a. S/H: *S* means Software based implementation, *H* means Hardware based implementation, like special instructions; b. CFLAG: GCC compilation flag; c. IEEE754 means algorithm exploits bits hacking of IEEE754 float format; d. Newton means Newton Iteration for sqrt.

There are many different implementations of the *sqrt* function for floating point numbers for AArch64 architecture. Software-based implementations include algorithms using Newton iteration and bits hacking of IEEE754 float representation. Hardware-based implementations include Arm VFP support for *fsqrt*, and Arm Neon support for float *sqrt*. Additionally, the performance of software-based implementations is also affected by the compilation flag. The default gcc compilation flag for TA is *-Os*, which optimizes space first; if we change it to *-O2*, the performance is more than 100x faster while the TA size increases from 55KB to 67KB. We evaluate all the above implementations by doing 3,200,000 sqrt operations and show the results in Table 4. Our TA initially used a software implementation using Newton Iteration algorithm. After evaluation, we switched to the Arm Neon based *sqrt* implementation for the speed and ease of implementation.

Appendix B Handling shortcuts in CNNs

Some CNNs contain shortcuts, such as ResNet [25] and InceptionNet [44], which create branches and merges of different convolution operations in its data-flow. The easiest way to handle it is to introduce a new operation called *TeeMerge* as shown in Fig 11. Unlike *TeeShadow* which takes only one input, *TeeMerge* can take multiple inputs and produce output for the corresponding convolution operation.

Appendix C Adversary’s Equivalent CNN

Figure 12 shows the original CNN, the ShadowNet transformed CNN and the adversary’s equivalent CNN.

Appendix D Security Analysis

Construction of Feasible Set: We refer to the kernels f_i in the random filter $F = [f_1, \dots, f_{m-n}]$ as mask kernels. Additionally, let \in_R represent a uniform random sampling. In what follows, we outline the methodology to compute the feasible set, $\mathcal{F}(\hat{W})$ for a given transformed weight matrix \hat{W} . The idea is to back-trace and compute the set of possible pre-images. Now, the feasible set is constructed as follows:

1. Select the set of $m - n$ indices uniformly at random:

$$\Omega \subset_R [m], |\Omega| = m - n \quad (22)$$

Ω represents a possible set of indices that correspond to the mask kernels.

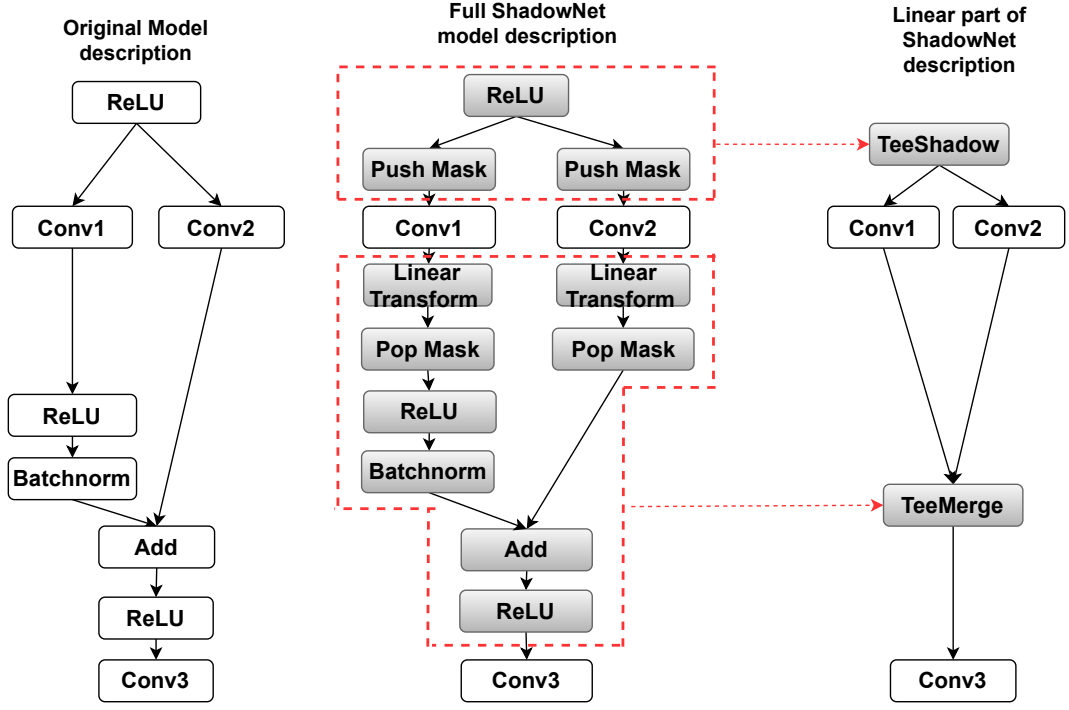


Figure 11: In the left part of the figure, a shortcut is introduced by Resnet (another convolution is removed from the left branch for simplicity). The middle figure shows the ShadowNet transformed model where the outputs from two different convolutions ($Conv1$ and $Conv2$) need to be merged. A new operation called *TeeMerge* is introduced here to take inputs from two branches and generate the corresponding output.

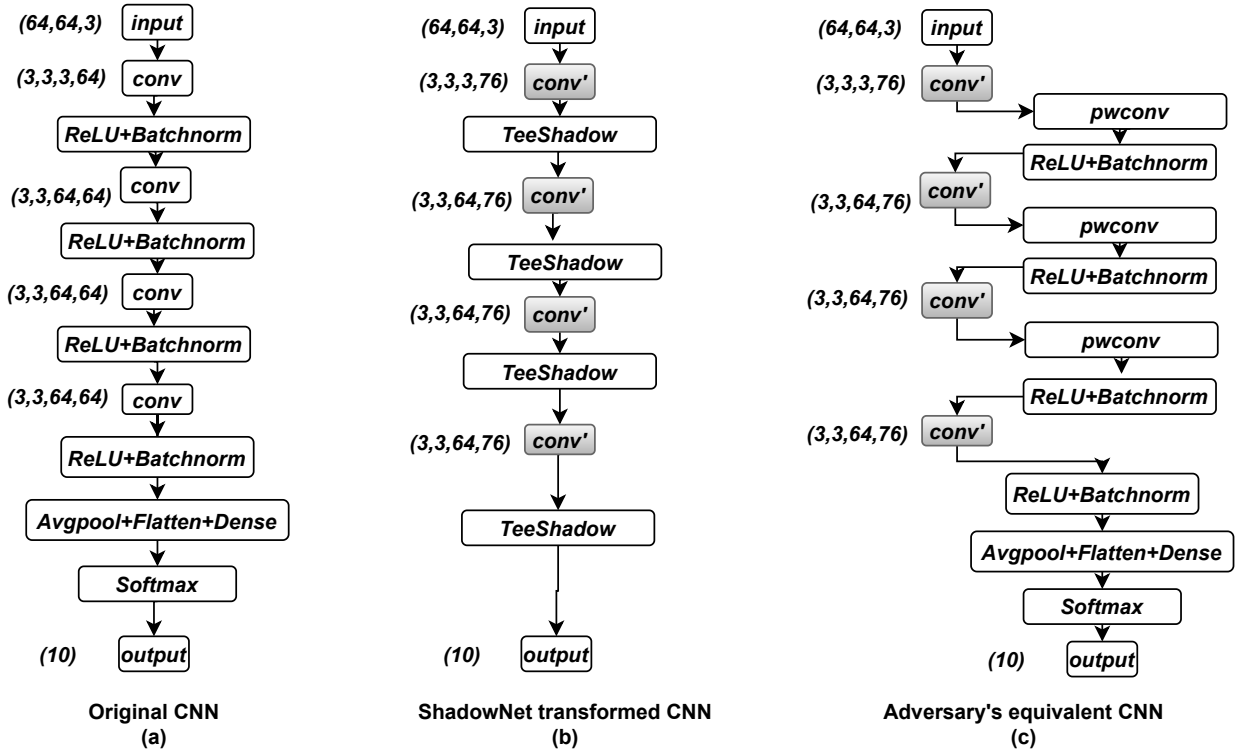


Figure 12: Figure (a) shows the original CNN model. Figure (b) is the ShadowNet transformed model. Figure (c) the adversary's equivalent CNN. Before training, its $conv'$ layers are initialized with weights copied from the corresponding $conv'$ layers of the ShadowNet transformed model. These $conv'$ layers are then reused by the adversary and marked as non-trainable during training.

2. The corresponding set of mask kernels is:

$$\Phi_\Omega = \{\hat{w}_i | i \in \Omega\} \quad (23)$$

3. Let $\bar{\Phi}_\Omega = \{\hat{w}_i | i \in [n] \setminus \Omega\}$ be the set of transformed original kernels. Additionally, let $\bar{W} = [\bar{w}_1, \dots, \bar{w}_n]$ where $\bar{w}_i \in \bar{\Phi}_\Omega$ and $\bar{w}_i \neq \bar{w}_j, i, j \in [n], i \neq j$.

4. Sample a random permutation $\sigma \in_R S_n$. We assume that $\sigma = \pi[1 : n]^{-1}$, i.e., σ reverses the effect of π on the transformed original kernels. Thus, $\bar{W}_\sigma = [\bar{w}_{\sigma(1)}, \dots, \bar{w}_{\sigma(n)}]$ represents a possible transformed filter.

5. Compute

$$\begin{aligned} & \forall i \in [n] \\ & \mathcal{F}_{\Omega, \sigma}^i(\hat{W}) = \{w | w = d \cdot (\bar{w}_{\sigma(i)} - \hat{w}'), d \in_R [-t, t], \hat{w}' \in_R \Phi_\Omega\} \end{aligned}$$

$\mathcal{F}_{\Omega, \sigma}^i(\hat{W})$ represents the set of possible values for the kernel w_i for the given Ω and σ .

6. Compute

$$\mathcal{F}_{\Omega, \sigma}(\hat{W}) = \{[w_1, \dots, w_n] | \forall i \in [n], w_i \in \mathcal{F}_{\Omega, \sigma}^i(\hat{W})\}$$

$\mathcal{F}_{\Omega, \sigma}(\hat{W})$ denotes the set of possible filters W for the given Ω and σ .

7. Clearly, we have

$$\mathcal{F}(\hat{W}) = \bigcup_{\Omega} \bigcup_{\sigma} \mathcal{F}_{\Omega, \sigma}(\hat{W}) \quad (24)$$

Clearly, larger the value of r , greater is the size of Ω and consequently, $\mathcal{F}(\hat{W})$. Additionally, it is evident that $\mathcal{F}(\hat{W}_a) \supset \mathcal{F}(\hat{W}_b)$ where $m_a = |\hat{W}_a| > |\hat{W}_b| = m_b$ (equivalently, $r_a > r_b$). For depthwise convolutional layer, we have

$$\mathcal{F}(\hat{W}) = \{[d_1 \cdot \hat{w}_{\sigma(1)}, \dots, d_n \cdot \hat{w}_{\sigma(n)}] | \sigma \in_R S_n, \forall i \in [n] d_i \in_R [-t, t]\} \quad (25)$$

Theorem 1. For a CNN with k convolutional layers and a given view of the normal world $\text{View}_{\text{Normal}} = (X_1, Y_k, \hat{W}_1, \dots, \hat{W}_k, X'_2, \dots, X'_k)$, we have:

$$\begin{aligned} & \forall i \in [k], \forall (W', W'') \in \mathcal{F}(\hat{W}_i) \times \mathcal{F}(\hat{W}_i) \\ & \Pr[W_i = W' | \text{View}_{\text{Normal}}] = \Pr[W_i = W'' | \text{View}_{\text{Normal}}] \end{aligned} \quad (26)$$

Proof. First, we present a helper lemma as follows.

Lemma 1. Adversary cannot reconstruct $W_i, i \in [n]$ from $(X_1, \hat{X}_2, \dots, \hat{X}_k, Y_k)$.

Proof. Recall that the goal of the adversary is to find W_i , i.e., solve for the $|W_i|$ variables. We assume that t is sufficiently large and that t is unknown to the adversary. Clearly, it is impossible for the adversary to unmask \hat{X}_i and figure out the exact values of X_i . Now, consider the first layer – the adversary has access to the true input X_1 but only gets to see the masked output $\hat{X}_2 = Y_1 + M_2$. In other words, adversary has $2|Y_1| + |W_i|$ unknown variables. Consequently, the adversary cannot

solve⁷ for the weights of W_1 from this. Similarly, for the last layer the adversary cannot solve for W_k from (\hat{X}_k, Y_k) . Now, for the other intermediate layers, both the input $(\hat{X}_i, i \in [2, k-1])$ and the output $(\hat{X}_{i+1} = Y_i + M_{i+1})$ is masked which clearly prevents solving for W_i . This concludes our proof for the above lemma. Note that here we assume the worst case situation for ShadowNet where $X_i = Y_{i-1}$. In practice, the adversary can only observe $\hat{X}_i = G(Y_{i-1}) + M_i$ where $G(\cdot)$ represents the non-linear layers. This adds additional complications for the adversary. For instance, negative values cannot be reversed for ReLU activation layers. \square

Clearly, from our construction of the feasible set in Equations (24) and (25), we have

$$\begin{aligned} \forall i \in [k], \forall (W', W'') \in \mathcal{F}(\hat{W}_i) \times \mathcal{F}(\hat{W}_i) \\ \Pr[W_i = W' | \hat{W}_i] = \Pr[W_i = W'' | \hat{W}_i] \end{aligned} \quad (27)$$

Equation (26) follows directly from Lemma 1 and Equation (27), concluding our proof. \square

⁷The input/output pair (X_i, Y_i) for any layer is connected to W_i by a system of linear equations. Hence, an adversary needs access to *both* the input and the output to solve for W_i